Octahedral tilting in $ACu_3Ru_4O_{12}$ (A = Na, Ca, Sr, La, Nd)

U. Schwingenschlögl *, V. Eyert, U. Eckern

Institut für Physik, Universität Augsburg, 86135 Augsburg, Germany

Abstract

The perovskite-like compounds $ACu_3Ru_4O_{12}$ (A = Na, Ca, Sr, La, Nd) are studied by means of density functional theory based electronic structure calculations using the augmented spherical wave (ASW) method. The electronic properties are strongly influenced by covalent-type bonding between transition metal d and oxygen p states. The characteristic tilting of the RuO_6 octahedra arises mainly from the Cu–O bonding, allowing for optimal bond lengths between these two atoms. Our results provide a deeper understanding of octahedral tilting as a universal mechanism, applicable to a large variety of multinary compounds.

1. Introduction

Despite its striking simplicity the perovskite structure, ABX_3, contains numerous crystallographic variations giving room for a huge class of compounds [1,2]. Among these the vast majority comprises oxides and fluorides [3], but also chlorides, hydrides, oxynitrides, and sulfides. The great interest in these materials is motivated by a variety of exciting dielectric, magnetic, electrical, optical, and catalytic properties, with several technological applications.

For optimal tailoring of materials much work on the perovskite-related compounds concentrates on the interrelations between deviations from the ideal perovskite structure and physical properties. These crystallographic deviations can be grouped into three different mechanisms [1,2]: While distortions of the characteristic BX_6 octahedra and cation displacements within the octahedra are mainly driven by electronic instabilities of the octahedral metal ion, octahedral tiltings represent the most common deviation and are observed when the A cation is too small for filling the space between regularly ordered octahedra. In this situation, octahedral tilting represents the lowest energy distortion, since it allows to adjust the A–O distances while leaving the first coordination sphere of the M cation intact, and changing mainly the soft M–O–M bond angle rather than the M–O bond length.

Of particular interest in this context are the perovskite-like compounds of the kind $AA'_3B_4O_{12}$, where the B–O–B bond angle is the relevant quantity in order to optimize both the A–O and A′–O bond lengths. Studying these materials thus promises deeper insight into the mechanisms

* Corresponding author. Fax: +49-821-598-3262.
E-mail address: udo.schwingenschloegl@physik.uni-augsburg.de (U. Schwingenschlögl).

driving the octahedral tilting. In addition, this material class shows extraordinary physical properties. While $CaCu_3Mn_4O_{12}$ is a ferromagnetic semiconductor with high Curie temperature and large magnetoresistance [4], $CaCu_3Ti_4O_{12}$ is known for its unusually high low-frequency dielectric constants [5–7]. In contrast, the metallic ruthenates of the type $ACu_3Ru_4O_{12}$ (A = Na, Ca, La) are Pauli paramagnets [8] and display valence degeneracy [7]. The crystal structures of the latter class have been studied recently by EXAFS and XRD, revealing considerable deviations of the measured interatomic distances from those expected from a bond valence approach [9].

The present study investigates the relationship between the octahedral tiltings and the electronic properties of the ruthenates $ACu_3Ru_4O_{12}$ (A = Na, Ca, Sr, La, Nd). The discussion is based on electronic structure calculations within density functional theory, which are known for their predictive power (see e.g., [10,11] and references therein). As a result, the specific bond lengths as well as the discrepancies between the experimental interatomic distances of the class $ACu_3Ru_4O_{12}$ and those proposed by the bond valance approach can be understood from the electronic properties and the type of chemical bonding.

2. Crystal structure

The compounds of the class $AA'_3B_4O_{12}$ crystallize in a body-centered cubic $2 \times 2 \times 2$ superstructure of the simple cubic perovskite structure with space group $Im\bar{3}$ (No. 204). The atoms are located at the following Wyckoff positions: A (2*a*) at $(0,0,0)$, A′ (6*b*) at $(\frac{1}{2},0,0)$, B (8*c*) at $(\frac{1}{4},\frac{1}{4},\frac{1}{4})$, and O (24*g*) at $(x,y,0)$. The crystal structure is shown in Fig. 1, where the BO_6 octahedra are easily identified. The tilting of the octahedra is controlled by the oxygen position, which, for all the ruthenates under study, is specified by $x_O \approx 0.175$ and $y_O \approx 0.305$. The deviation from the ideal values $x_O = y_O = 0.25$ causes a rotation of the octahedra around the [1 1 1] axis. As a consequence, the A sites are partitioned into the A site at $(0,0,0)$ and the A′ site, which takes three quarters of the original A positions. In particular, the A′ sites are strongly affected by the oxygen atom shifts away from the ideal position and thus their surrounding experiences the largest distortion. As a consequence, three different A′–O distances of ≈2.0, 2.8, and 3.2 Å appear, each forming an approximately square-planar coordination and thus providing an ideal geometry for a Jahn–Teller active ion as e.g., Cu^{2+} [9]. The CuO_4 squares can be easily identified in Fig. 1.

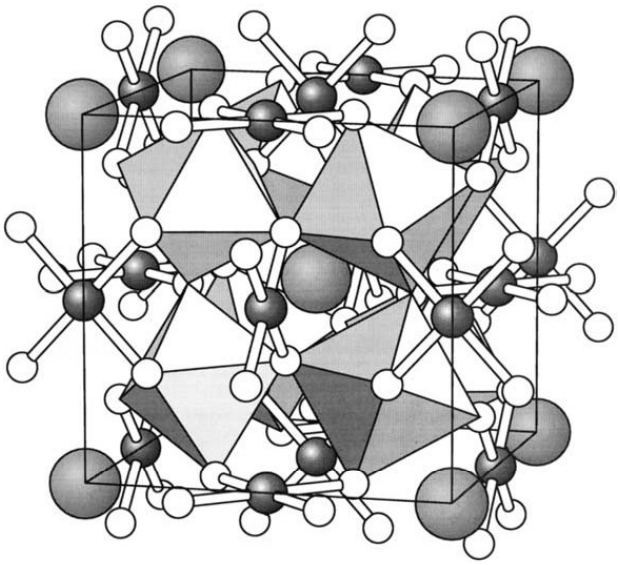

Fig. 1. Crystal structure of $AA'_3B_4O_{12}$. Large and medium size spheres denote A- and Cu-atoms, respectively, while octahedra represent the BO_6 units.

For the ruthenates $ACu_3Ru_4O_{12}$ (A = Na, Ca, Sr, La, Nd) studied in the present work, crystallographic data were determined by Ebbinghaus et al. [9]. The lattice constants are similar to those reported by Labeau et al. [8] as well as Subramanian and Sleight [7]. Both the lattice constants and oxygen parameters of these compounds show only slight deviations and amount to $a \approx 7.4$ Å as well as $x_O \approx 0.175$ and $y_O \approx 0.305$ as mentioned above.

3. Method of calculation

The electronic structure calculations were performed within the framework of density functional theory and the local density approximation using the augmented spherical wave (ASW) method

[12,13]. In order to represent the correct shape of the crystal potential in the large voids, additional augmentation spheres were inserted into the open crystal structures. Optimal augmentation sphere positions as well as radii of all spheres were found automatically by the sphere geometry optimization (SGO) algorithm [14]. The basis sets comprised Cu 4s, 4p, 3d; Ru 5s, 5p, 4d, 4f, and O 2s, 2p as well as states of the additional augmentation spheres. In addition, Na 3s, 3p, 3d; Ca 4s, 4p, 3d, 4f; Sr 5s, 5p, 4d, 4f; La/Nd 6s, 6p, 5d, 4f states were used for the A cation. The Brillouin zone sampling was done using an increasing number of **k** points within the irreducible wedge ranging from 17 to 1255 points to ensure convergence of the results with respect to the **k**-space grid. In addition to the analysis of the (partial) densities of states we will also address the question of chemical bonding in terms of the covalent bond energy, which was recently proposed [15] as an extension to the concept of the crystal orbital overlap population (COOP) [16]. In short, the covalent bond energy covers those contributions to the total energy of a crystal, which arise from the hybridization of orbitals located at different atoms.

4. Results and discussion

Partial densities of states (DOS) for all five compounds under consideration are displayed in Fig. 2. The electronic structure in the energy window shown is dominated by Cu 3d, Ru 4d, and O 2p states. In addition, Nd 4f states cause a sharp peak at and slightly above E_F for $NdCu_3Ru_4O_{12}$. The gross features are very similar for all compounds. Three energy ranges can be distinguished. In the broad interval from about −8 to −3 eV oxygen 2p states dominate but are complemented by considerable contributions from the transition metal d states due to covalent bonding. Whereas in the energy range from −3 to −2 eV a sharp Cu 3d peak appears, electronic states between −2 and 0.5 eV, and hence metallic conductivity, derive mainly from broader Ru 4d bands. Covalent-type bonding leads to finite oxygen 2p contributions above −3 eV. This is confirmed by covalent bond energy curves calculated for the sodium compound as shown in Fig. 3. Both the Cu–O and the Ru–O curves are negative and positive at energies below and above −3 eV, respectively, indicative of bonding and antibonding states in the energy regions, where the O 2p and the transition metal d states dominate. However, due to the higher d electron count of Cu as compared to Ru, the Cu–O antibonding states are filled, leading to a vanishing contribution of these bonds to the chemical stability. In contrast, the integrated Ru–O covalent bond energy curve at E_F has a finite value indicative of the stabilizing net contribution of this bond. Finally, metal–metal bonding results in small peaks between −3 and −2 eV and above the Fermi energy.

All states which are not displayed in Fig. 2 play only a very small role in the energy interval shown. In particular, apart from the Nd 4f states, the A cation electrons do not contribute to the covalent-type bonding but are distributed over the solid. As a consequence, changes at the A cation site show up mainly in the modified total electron count.

Ebbinghaus et al. [9] related the measured atomic distances for $ACu_3Ru_4O_{12}$ (A = Na, Ca, Sr, La, Nd) to the predictions of the bond valence model. The latter is an empirical model, which connects the valences and the mutual distances of the atoms [17]. It starts out from ionic configurations but looses accuracy in covalently bonded crystals. For the divalent A cations the Ru–O distances were found to agree with the expected values. In the case of A = Na the bond length is longer, while for A = La, Nd it is shorter than predicted by the bond valence model.

In order to understand the influence of octahedral tilting on the electronic properties and to analyze the mentioned discrepancies reported by Ebbinghaus et al. we performed additional calculations using hypothetical crystal structures. In these setups the oxygen atoms were shifted away from the measured positions to the ideal position $x_O = 0.25$, $y_O = 0.25$ and to $x_O = 0.15$, $y_O = 0.35$. These positions correspond to zero tilting of the octahedra and to an exaggerated tilting, respectively. Note that shifting the oxygen position mainly affects the Cu–O bond lengths, while the effect for the Ru–O and A–O distances is of second order. The partial DOS for the hypothetical structures of $NaCu_3Ru_4O_{12}$ are displayed in Fig. 4. Considerable

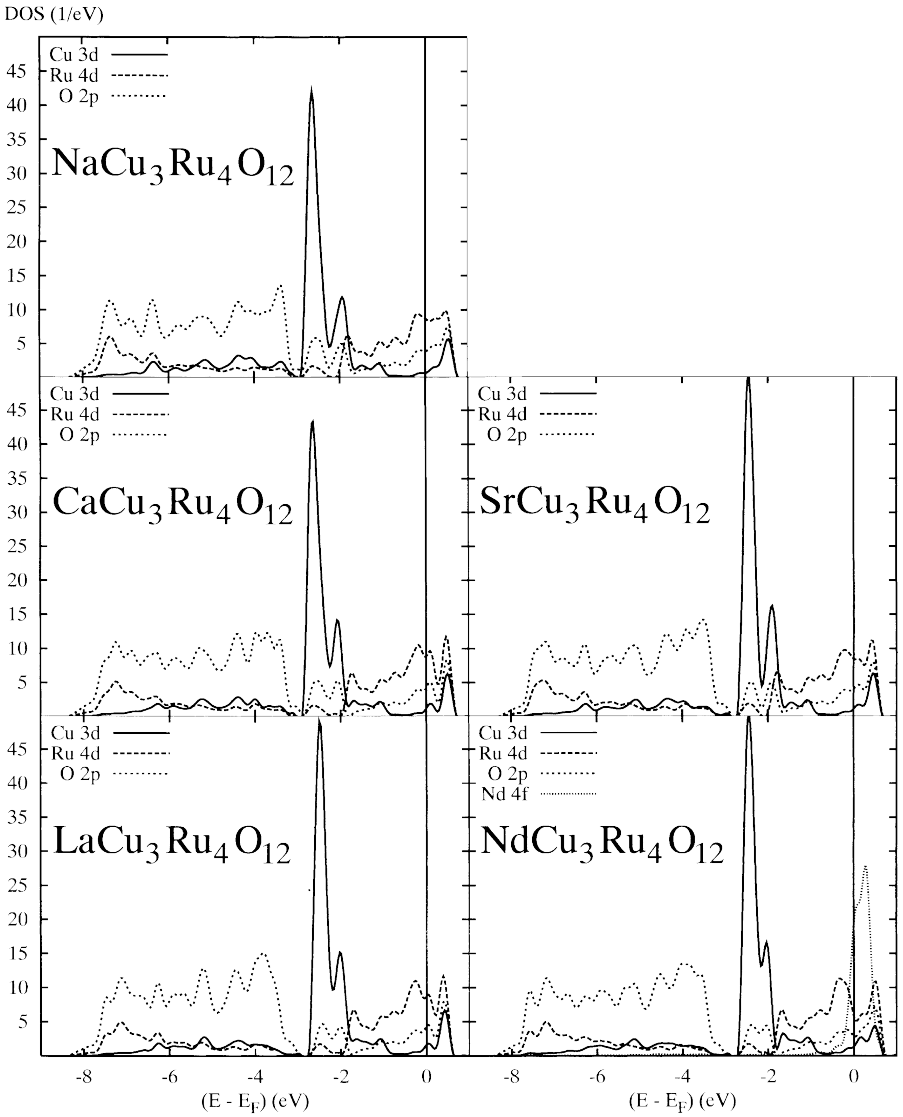

Fig. 2. Partial Cu 3d, Ru 4d, and O 2p densities of states (DOS) of $ACu_3Ru_4O_{12}$ per formula unit. 4f states have been included for the Nd-compound.

changes as compared to the results for the experimental crystal structure (see Fig. 2) are observed. Turning to the ideal structure first, we observe (i) a considerable broadening of the O 2p dominated states and (ii) a striking sharpening of the Cu 3d states. Both effects are readily understood from the oxygen shifts. The latter cause an increase of the Cu–O distances and, to a lesser degree, a decrease of the Ru–O distances, leading to a slightly larger 2p–4d overlap. As a consequence, larger Ru 4d contributions at energies below −3 eV are observed, whereas the Cu 3d fraction is almost negligible in this region. At the same time, Ru 4d and O 2p admixture to the sharp Cu 3d peak is likewise very small. To sum up, shifting the oxygen atoms to their ideal positions leads to an effective decoupling of the compound into RuO_6 octahedra and Cu atoms, which are effectively separated and thus do no longer form a stable solid.

On the contrary, for the hypothetical structure with the oxygen shift away from the ideal position exaggerated (i) the oxygen states have moved to lower energies and (ii) the Cu 3d states do no longer form a distinct peak but have attained a rather

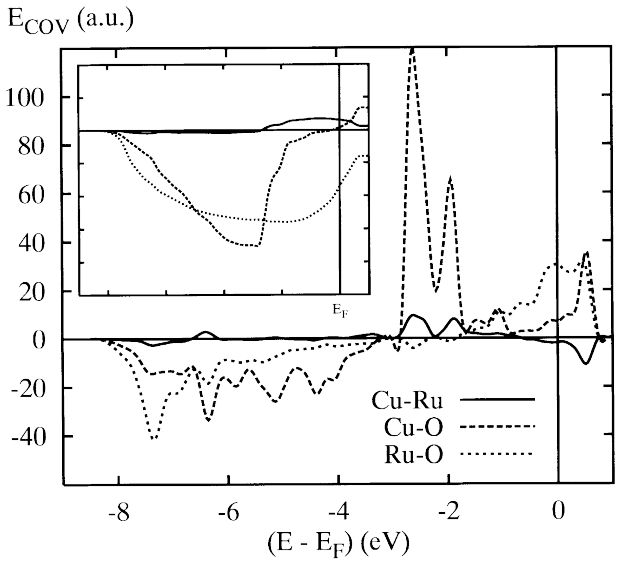

Fig. 3. Covalent bond energy curves for $NaCu_3Ru_4O_{12}$. The corresponding integrated covalent bond energies are given in the inset.

itinerant character. The latter goes along with an increased similarity of the Cu 3d and O 2p partial DOS. The increased covalent-type bonding between these two states is also reflected by large contributions to the covalent bond energy (not shown), negative below –4 eV and positive above, leading to a net antibonding integral at E_F. The increased 2p–3d bonding is in contrast to a slight decrease of the bonding between the Ru 4d and O 2p states due to the larger extension of the RuO_6 octahedra. Thus the hypothetical structure with exaggerated oxygen shifts likewise suffers from an increase of antibonding at the expense of bonding states.

Together with the instability of the hypothetical structure with ideal oxygen positions we conclude that the experimental structure is due to an optimal balance of different types of bonds, namely 2p–3d and 2p–4d. This balance is less affected by the A cations, which do not take part in covalent bonding but have lost their outer electrons. For this reason, from the point of view of chemical bonding, there is no means to optimize the A–O bond length. Moreover, as for the Ru–O distance, the A–O distance is only to a small degree affected by the tilting. Finally, the different types of bonding present in these compounds give an additional explanation for the deviations of the experimental interatomic distances from those expected from the bond valence model.

5. Conclusions

The electronic properties of the perovskite-like ruthenates $ACu_3Ru_4O_{12}$ are governed by strong covalent bonding between the transition metal d and the oxygen 2p electrons. While Ru–O bonds via the corresponding bond lengths influence mainly the size of the octahedra and hence the lattice constant, the octahedral tilting is to a large part due to the Cu–O bonding.

As compared to the ideal perovskite structure the tilting of the characteristic RuO_6 octahedra has

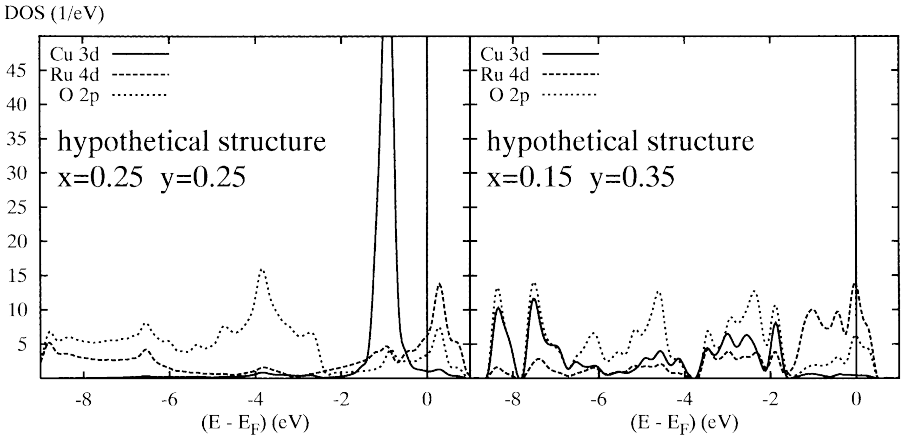

Fig. 4. Partial Cu 3d, Ru 4d, and O 2p densities of states (DOS) of hypothetically distorted variants of $NaCu_3Ru_4O_{12}$ per formula unit.

only little effect on the Ru–O bonding. In contrast, the Cu–O distances undergo serious changes, leading eventually to the square-planar coordination of copper. Finally, the unusual A–O distances and the failure of the bond valence approach are due to the fact that their response to the tilting is only small and the structure does not offer any possibility to simultaneously optimize the A–O and the Cu–O bond lengths.

In conclusion, octahedral tilting as discussed for $ACu_3Ru_4O_{12}$, arises from the interplay of covalent bonding between different atomic species, leading to optimized bond lengths between all atoms involved. This general principle is of rather universal nature and applies to a large variety of compounds.

Acknowledgements

Fruitful discussions with S.G. Ebbinghaus and A. Weidenkaff are gratefully acknowledged. This work was supported by the Deutsche Forschungsgemeinschaft through SFB 484.

References

[1] P.M. Woodward, Acta Crystallogr. B 53 (1997) 32.
[2] P.M. Woodward, Acta Crystallogr. B 53 (1997) 44.
[3] J.B. Goodenough, J.M. Longo, in: Landolt-Börnstein, Series III, vol. 4A, 1970, p. 126.
[4] Z. Zeng, M. Greenblatt, M.A. Subramanian, M. Croft, Phys. Rev. Lett. 82 (1999) 3164.
[5] M.A. Subramanian, D. Li, N. Duan, B.A. Reisner, A.W. Sleight, J. Solid State Chem. 151 (2000) 323.
[6] C.C. Homes, T. Vogt, S.M. Shapiro, S. Wakimoto, A.P. Ramirez, Science 293 (2001) 673.
[7] M.A. Subramanian, A.W. Sleight, Solid State Sci. 4 (2002) 347.
[8] M. Labeau, B. Bochu, J.C. Joubert, J. Chenavas, J. Solid State Chem. 33 (1980) 257.
[9] S.G. Ebbinghaus, A. Weidenkaff, R.J. Cava, J. Solid State Chem. 167 (2002) 126.
[10] J. Kübler, V. Eyert, in: K.H.J. Buschow (Ed.), Electronic and Magnetic Properties of Metals and Ceramics, VCH Verlagsgesellschaft, Weinheim, 1992, pp. 1–145, in: R.W. Cahn, P. Haasen, E.J. Kramer (Eds.), Volume 3A of the Series: Materials Science and Technology, VCH Verlagsgesellschaft, Weinheim, 1991–1996.
[11] V. Eyert, in: M. Springborg (Ed.), Density Functional Methods: Applications in Chemistry and Materials Science, Wiley, Chichester, 1997, p. 233.
[12] A.R. Williams, J. Kübler, C.D. Gelatt Jr., Phys. Rev. B 19 (1979) 6094.
[13] V. Eyert, Int. J. Quantum Chem. 77 (2000) 1007.
[14] V. Eyert, K.-H. Höck, Phys. Rev. B 57 (1998) 12727.
[15] N. Börnsen, B. Meyer, O. Grotheer, M. Fähnle, J. Phys. Condens. Mater. 11 (1999) L287.
[16] R. Hoffmann, Solids and Surfaces: A Chemist's View of Bonding in Extended Structure, VCH, New York, 1988.
[17] I.D. Brown, D. Altermatt, Acta Crystallogr. 41 (1985) 244.